Moderate GSK-3β inhibition improves neovascular architecture, reduces vascular leakage, and reduces retinal hypoxia in a model of ischemic retinopathy

Mien V. Hoang,
Department of Pathology and Center for Vascular Biology Research, Beth Israel Deaconess Medical Center and Harvard Medical School, 99 Brookline Avenue, Boston, MA 02215, USA

Lois E. H. Smith, and
Department of Ophthalmology, Children's Hospital Boston and Harvard Medical School, Boston, MA 02115, USA

Donald R. Senger
Department of Pathology and Center for Vascular Biology Research, Beth Israel Deaconess Medical Center and Harvard Medical School, 99 Brookline Avenue, Boston, MA 02215, USA

Abstract

In ischemic retinopathies, unrelieved hypoxia induces the formation of architecturally abnormal, leaky blood vessels that damage retina and ultimately can cause blindness. Because these newly formed blood vessels are functionally defective, they fail to alleviate underlying hypoxia, resulting in more pathological neovascularization and more damage to retina. With an established model of ischemic retinopathy, we investigated inhibition of glycogen synthase kinase-3β (GSK-3β) as a means for improving the architecture and functionality of pathological blood vessels in retina. In vitro, hypoxia increased GSK-3β activity in retinal endothelial cells, reduced β-catenin, and correspondingly impaired integrity of cell/cell junctions. Conversely, GSK-3β inhibitors restored β-catenin, improved cell/cell junctions, and enhanced the formation of capillary cords in three-dimensional collagen matrix. In vivo, GSK-3β inhibitors, at appropriately moderate doses, strongly reduced abnormal vascular tufts, reduced abnormal vascular leakage, and improved vascular coverage and perfusion during the proliferative phase of ischemia-driven retinal neovascularization. Most importantly, these improvements in neovasculature were accompanied by marked reduction in retinal hypoxia, relative to controls. Thus, GSK-3β inhibitors offer a promising strategy for alleviating retinal hypoxia by correcting key vascular defects typically associated with ischemia-driven neovascularization.

Keywords

Retinopathy; Neovascularization; Glycogen synthase kinase-3β; Hypoxia; Endothelial cell; β-catenin

Introduction

Hypoxia induces neovascularization in retina largely through the HIF-regulated angiogenic cytokine VEGF [1-7]. However, such neovascularization is typically defective both architecturally and functionally. Poor architectural integrity is responsible for increased vascular leakage, hemorrhage, and poor blood flow; and all of these features are the characteristic of VEGF-induced neovascularization [8]. Persistently poor perfusion and flow fails to relieve hypoxia, resulting in more pathological neovascularization. Ultimately, the combination continued abnormal neovascularization, hemorrhage, vessel leakiness, poor perfusion, and prolonged hypoxia contribute to vision loss. Thus, the architectural and functional defects associated with ischemia-driven neovascularization in retina are an important clinical problem.

The reasons why ischemia and VEGF do not induce formation of vasculature with normal architecture and function are complex and unclear. However, it is likely that the abnormal neovessels lack the proper balance of signals that govern the ordered assembly of microvascular endothelial cells (MVECs) into three-dimensional vascular networks with intact vessel barrier function. In other words, the structural and functional abnormalities in ischemia-induced neovessels are a likely consequence of defective vascular morphogenesis. Guided by this hypothesis, we have sought to identify pharmacological strategies for correcting defects in vascular morphogenesis commonly associated with hypoxia-driven angiogenesis; and, in particular, we investigated inhibitors of glycogen synthase kinase-3β (GSK-3β). Although initially described as a key enzyme involved in glycogen metabolism, GSK-3β is now recognized to regulate numerous cell functions including cytoskeletal dynamics [9,10] and β-catenin—an important regulator of endothelial cell/cell junctions and nuclear transcription [11,12]. Importantly, inhibition of GSK-3β has been shown to promote angiogenesis in a Matrigel plug assay [13] and also in models of myocardial infarction [12,14]. Moreover, GSK-3β is expressed in retina [15], suggesting that the modulation of GSK-3β activity during abnormal retinal angiogenesis warrants investigation. As described here, with an established mouse model of ischemic retinopathy, we found that administration of moderate doses of three distinctly different GSK-3β inhibitors markedly improved new blood vessel architecture and perfusion, ultimately reducing vascular leakage and improving retinal oxygenation.

Methods

Oxygen-induced retinopathy

All protocols involving mice were approved by the Beth Israel Deaconess Medical Center Institutional Animal Care and Use Committee. Retinopathy was induced by exposing 7-day-old (P7) C57BL/6 pups with their nursing mother (Jackson Laboratory) to 75% oxygen (hyperoxia) for 5 days to induce >95% vaso-obliteration of the retinal vessels as previously described [16]. At day 12 (P12), the pups and the mother were returned to normal room air (21% oxygen), resulting in hypoxic retina and re-growth of new blood vessels. GSK-3β inhibitor VIII (AR-A014418), GSK-3β inhibitor I (TDZD-8), and cell-permeable GSK-3β peptide inhibitor L803-mts (Myr-N-GKEAPPAPPQSpP-NH$_2$), or control vehicle were administered daily by intraperitoneal injection from days P12 to P16 or from days P12 to P20, as indicated, with animals harvested at day P17 or P21 for the evaluation of retinal blood vessel architecture and function (below). Unless indicated otherwise, standard daily doses were as follows: GSK-3β inhibitor VIII (10 mg/kg), GSK-3β inhibitor I (3.0 mg/kg) and cell-permeable GSK-3β peptide inhibitor (0.5 mg/kg). All were purchased from EMD Biosciences.

Analyses of retinal vascular coverage, vascular leakiness, vascular perfusion, and hypoxia

Animals were killed, eyes enucleated, whole mount retinas prepared for analyses as described [17] with the following additions/modifications. Following the fixation for 1 h in 10% formalin at room temperature, retinas were dissected, washed in PBS (three times), blocked, and permeabilized overnight in PBS buffer containing 0.5% Triton X-100, 10% goat serum, and 0.02% sodium azide. For analyses of vascular coverage, retinas were stained with TRITC-Lectin from *Bandeiraea simplicifolia* (Sigma). Analyses of vascular perfusion and leak were performed employing lysine-fixable 70-kDa FITC-dextran (10 mg/kg, Invitrogen) injected via the tail vein in live animals. Animals were harvested after 10-min perfusion. To assess retinal hypoxia, Hypoxyprobe™-1 (pimonidazole 120 mg/kg, Hypoxyprobe, Inc. Burlington, MA) was used instead of FITC-dextran, and it was administered 1 h before harvest. Retinas were co-stained with FITC-Hypoxyprobe antibody and *Bandeiraea simplicifolia* TRITC-Lectin for assessment of hypoxia and vasculature, respectively. Stained retinas were visualized and photographed with a camera Leica DX-300 microscope using 4×, 10× and 20× objectives.

Vascular parameters were quantified from digital images of whole retinas. Measurement of retinal neovascularization (vascular coverage and perfused neovasculature) and neovascular tuft formation was taken as described previously [18]. Briefly, images were imported into Adobe Photoshop; avascular areas, perfused vascular areas, and neovascular tuft areas each were quantified by comparing the number of pixels in the affected areas with the total number of pixels in the retina. Focal leakage points were identified as "clouds" of 70 kDa FITC-dextran outside of vasculature and counted manually. Hypoxia was quantified by measuring hypoxic area and integrating measured hypoxic area with FITC-Hypoxyprobe signal intensity.

Immunohistochemical staining of vascular tufts in cross section

Eyes were enucleated, embedded in OCT medium, and snap frozen in liquid nitrogen. Five-micron thick sections were cut and endothelial cells stained with CD31 (PECAM-1) antibody (Pharmingen) followed by secondary antibody conjugated with horseradish peroxidase. Antibody staining was visualized with DAB substrate, and sections were counterstained with hematoxylin solution.

In vitro analyses of human retinal MVECs: capillary morphogenesis in 3D collagen-I, staining for F-actin, treatment with hypoxia, analyses of GSK-3*β* activity and *β*-catenin

Cells and capillary morphogenesis assays—Human retinal microvascular endothelial cells (retinal MVECs, Cell-Systems) were propagated in corresponding CS-C Complete Medium Kit (Cell-systems) and used between passages three and seven. Capillary morphogenesis assays were performed by "sandwiching" confluent cell monolayers with rat tail collagen-I (BD Biosciences), basically as described previously [19]. The assay was performed in 12-well plates with 1.0 mg/ml collagen-I in full medium. GSK-3*β* inhibitors at various concentrations or vehicle were added for overnight incubation, prior to adding the upper layer of collagen-I. Capillary morphogenesis was allowed to proceed for 16 h; the assay plates were fixed with 10% formalin for 1 h and stained for F-actin with fluorescent Oregon Green-conjugated phalloidin (Invitrogen, final concentration 0.5 units/ml) and subsequently photographed. Cord length, blind ends, and polygons were quantified using NIH ImageJ software. Cord length was traced and measured through freehand line selections. Blind ends and polygons were determined with point selections. Measured parameters correspond to actual areas of 0.8 mm^2.

Hypoxia, GSK-3β activity, and β-catenin—Retinal MVECs were grown to confluence in full medium. Medium was changed to serum-free basal medium containing 2% fetal

bovine serum overnight, and cells were subjected to hypoxia (5% oxygen) for the indicated time followed by harvest in lysis buffer (20 mM Tris-HCl, 150 mM NaCl, 10% Glycerol, 1% Nonidet P-40, 3 mM $MgCl_2$, 1 mM EDTA, 1 mM EGTA, 25 mM NaF, 5 mM Na_3VO_4, 150 μM sodium pyrophosphate, and a cocktail of protease inhibitors containing 4-(2-aminoethyl)benzenesulfonyl fluoride (AEBSF), pepstatin A, E-64, bestatin, leupeptin, and aprotinin. Lysates (20 μg protein) were subjected to electrophoresis with SDS–PAGE on 4–20% gradient gel and electrophoretically transferred to PVDF membrane (BIO-RAD). For analyses of GSK-3β or β-catenin, blots were stained with GSK-β Ser[9] phosphospecific antibody (Cell Signaling, cat. #9336) or β-catenin antibody (BD Signal Transduction Laboratories), respectively; and protein bands were detected with ECL Western blotting substrate. For GSK-3β analyses, the membrane was stripped and re-stained with total GSK-3β antibody (Cell Signaling, cat. #9315). Band intensities were quantified with a digital scanner. For β-catenin analyses, the membrane was stripped and re-stained with polyclonal antibody to total Erk1/Erk2 as a loading control. We have found this loading control to be particularly suitable for MVECs under a variety of conditions [20,21].

Immunohistochemical staining of β-catenin in vascular cords—GSK-3β inhibitors were added and incubated with cells in 24-well plates overnight. The next day, each well was overlaid, rather than "sandwiched" (as above), with 300 μl of collagen-I at concentration of 0.25 mg/ml in CS-C Medium (minus serum and growth factors, Cell-Systems), together with GSK-3β inhibitors as indicated. Capillary morphogenesis was allowed to proceed for 6 h under normoxic or hypoxic conditions; and cells were fixed in 10% formalin for 10 min, permeabilized for 1 min with 0.02% Triton-X100 in PBS and stained with antibody to β-catenin (BD Signal Transduction Laboratories) followed by Alexa Fluor 610 secondary antibody (Invitrogen).

Statistical analysis

Findings are presented as mean ± standard error. Statistical analyses were performed with InStat 3 software for Macintosh. For comparisons between two groups, we employed the two-tail Mann–Whitney test, assuming unequal variances between the two groups under comparison. For comparisons among multiple groups, data were analyzed with ANOVA, followed by the Bonferroni post-test.

Results

Hypoxia increases GSK-3β activity in retinal MVECs with loss of β-catenin from cell/cell junctions

To investigate potential relationships between GSK-3β activity and hypoxia that is typical of ischemic retinopathy, we evaluated GSK-3β activity in isolated human retinal MVECs subjected to hypoxia (5% O_2) in vitro. Hypoxia increased GSK-3β activity significantly, as indicated by a greater than 50% reduction in phosphorylation of the GSK-3β Ser[9] residue [22] (Fig. 1a, b). Moreover, as determined with immunoblotting of whole retinal MVEC lysates, hypoxia greatly reduced β-catenin that is targeted for degradation by active GSK-3β [11] (Fig. 1c). Consistent with the loss of β-catenin due to GSK-3β activation, GSK-3β inhibitor VIII (AR-A014418) [23] restored β-catenin (Fig. 1c). Finally, as determined with immunohistochemistry, hypoxia also reduced β-catenin at cell/cell junctions in retinal MVECs undergoing collagen-induced capillary morphogenesis in vitro, whereas GSK-3β inhibitor VIII increased β-catenin at cell/cell junctions (Fig. 1d). Thus, to summarize, these experiments establish that retinal MVECs express GSK-3β, GSK-3β is activated in retinal MVECs by hypoxia, and activation of GSK-3β in retinal MVECs corresponds to a marked loss of β-catenin that can be reversed by GSK-3β inhibitor.

Identification of GSK-3β inhibitors as compounds that improve capillary morphogenesis of retinal MVECs in vitro

We also investigated the consequences of inhibiting GSK-3β for capillary morphogenesis in an established in vitro model performed by "sandwiching" confluent retinal MVECs between two layers of interstitial collagen type I, thereby provoking organization into solid pre-capillary cords that are the precursors to capillary-like tubes with lumens (reviewed in [24]). The strong predictive value of this in vitro assay for the identification of compounds that improve neovascular architecture in vivo is supported by our previous work with RhoA GTPase mutants [25]. At moderate doses, GSK-3β inhibitor VIII [23], GSK-3β inhibitor I (TDZD-8) [26], and cell-permeable GSK-3β peptide inhibitor (Myr-N-GKEAPPAPPQSpP-NH$_2$) [27] each improved the organization of retinal MVECs into capillary cords—as measured by increased cord length, reduced blind ends, and overall network organization (polygons) (Fig. 2a, b). In all cases, appropriate inhibitor dose was critical because higher doses of inhibitor interfered with capillary morphogenesis (Fig. 2c). Nonetheless, these in vitro assays together with findings presented in Fig. 1 identified GSK-3β inhibitors, at appropriate doses, as candidates for improving capillary morphogenesis of retinal MVECs in vivo.

Testing of GSK-3β inhibitors in a mouse model of ischemic retinopathy: improved vascular coverage, reduction of abnormal vascular tufts, reduced vascular leak, and improved retina perfusion

Given the promising in vitro findings described above, we tested GSK-3β inhibitors in an established model of retinopathy in neonatal mice that exhibits vascular defects typically associated with ischemic retinopathies [16]. In this model, immature retinal blood vessels are obliterated in 7-day-old (P7) mice with hyperoxia (75% O$_2$) for 5 days. At day P12, animals are returned to room air, resulting in retinal hypoxia and increased VEGF expression [7,28,29] that induces abnormal revascularization [30]. Because the in vitro experiments described above suggested that inhibitor dose is critical, we initially performed a series of experiments to test a range of GSK-3β inhibitor doses, in order to define optimum doses for further testing. As shown in Fig. 3, moderate doses of GSK-3β inhibitor VIII (AR-A014418), GSK-3β inhibitor I (TDZD-8), and GSK-3β cell-permeable peptide inhibitor L803-mts (Myr-N-GKEAPPAPPQSpP-NH$_2$) each improved vascular re-growth with 5 days of treatment (Fig. 3a, b). Similar to findings in vitro, each inhibitor provided improvement within a limited dose range; higher doses failed to improve vascular coverage (Fig. 3c). We observed no evidence of deleterious effects on animal health with any of these drugs at the doses employed to improve vascular re-growth.

Next, we examined the effects of GSK-3β inhibitor treatment on formation of abnormal vascular tufts—a key defect in vascular architecture associated with ischemic retinopathy [16]. Again, animals were treated for 5 days, from P12 to P17. At doses that provided improved vascular re-growth and coverage of retina (Fig. 3), GSK-3β inhibitor VIII (AR-A014418), GSK-3β inhibitor I (TDZD-8), and GSK-3β cell-permeable peptide inhibitor (L803-mts) each markedly reduced the formation of prominent abnormal vascular tufts, as determined with immunohistochemical staining of retinal vasculature in cross section (Fig. 4a, b). Similarly, these GSK-3β inhibitors sharply reduced focal leakage in retina, as determined with FITC-dextran tracer (Fig. 5a, b). In untreated animals, vascular leaks were often associated with abnormal vascular tufts; and therefore, reduction in focal leaks by GSK-3β inhibitors is consistent with the associated reduction in abnormal vascular tufts. In summary, treatment with appropriate doses of GSK-3β inhibitors for 5 days (P12–P17) improved vascular re-growth and coverage of retina (Fig. 3), markedly reduced abnormal vascular tufts (Fig. 4), and markedly reduced vascular leakage (Fig. 5). Moreover, very similar improvement in all categories was achieved with three different GSK-3β inhibitors

with distinctly different chemistries. Importantly, after 5 days treatment, these significant vascular improvements were achieved together with significant increases in functional vasculature, as determined by perfusion with FITC-dextran tracer (Fig. 6a, b).

Treatment with GSK-3β inhibitors for 9 days (P12-P21): continued improvement in vascular coverage and substantial reduction in retinal hypoxia

As illustrated in Figs. 3, 4, 5, and 6, vascular architectural and functional improvements achieved with GSK-3β inhibitors were highly significant after 5 days of treatment (P17); however, vascular coverage and perfusion of retina was still incomplete (Figs. 3 and 6). Therefore, we performed additional experiments in which treatment with GSK-3β inhibitors was increased to 9 days, covering the time period from the onset of retinopathy to P21. At P21, vascular coverage of retina in GSK-3β inhibitor groups was nearly complete and ≥ 50% improved relative to the control group (Fig. 7a, b). Consistent with improved vascular coverage, we expected that GSK-3β inhibitors also would reduce retinal hypoxia and restore oxygenation of retina to normal levels, a key therapeutic goal. To test this possibility directly, we employed an established immunohistochemical method (Hypoxyprobe™, pimonidazole HCl). With 9 days of treatment (P12–P21), GSK-3β inhibitors strikingly reduced retinal hypoxia by ~75% relative to controls, and this reduction in retinal hypoxia correlated closely with improved neovascularization (Fig. 7b, c).

Discussion

In ischemic retina, hypoxia drives pathological neovascularization [1,3-7]. Logically, neovascularization should relieve hypoxia; but the architectural defects and vascular leakiness typically associated with pathological neovascularization result in poor blood flow and persistent hypoxia [8]. Unrelieved hypoxia and persistent pathological neovascularization damage retina and ultimately cause blindness [1,2,31]. Accordingly, a desirable therapeutic strategy should correct the vascular abnormalities associated with pathological neovascularization and also alleviate hypoxia. As shown here, systemic daily administration of appropriate doses of GSK-3β inhibitors to neonatal mice with proliferative ischemic retinopathy improves neovascular coverage of retina, reduces abnormal vascular tufts, reduces vascular leak, and improves vascular perfusion of retina. Most importantly, these improvements in neovasculature reduce retinal hypoxia, consistent with improved vascular function. Thus, GSK-3β inhibitors offer a promising strategy for treating ischemic retinopathies by correcting key architectural and functional defects associated with hypoxia-driven neovascularization.

Apart from optimal doses, we observed no differences in overall effectiveness of the different GSK-3β inhibitors. Other than possible interactions with the closely related α isoform [22], the GSK-3β inhibitors employed are highly selective; and each acted similarly despite markedly different chemistries and distinctive modes of action. Moreover, all three inhibitors were used at relatively low concentration, which favors selectivity. GSK-3β inhibitor VIII is a cell-permeable thiozole-containing urea compound that acts through competition with ATP [23], GSK-3β inhibitor I is a cell-permeable thiadiazolidinone analog that blocks GSK-3β independently of ATP binding [26], and GSK-3β cell-permeable peptide inhibitor L803-mts acts by binding to the substrate pocket [27]. GSK-3β inhibitor VIII is ~1,000× more selective for GSK-3 than other kinases [23]; and, apart from GSK-3α, GSK-3β inhibitor I [26] and GSK-3β cell-permeable peptide inhibitor L803-mts [27] do not inhibit other kinases detectably. Thus, the specificity of these inhibitors, the relatively low doses employed, and the differences in their modes of action make it highly probable that the effects we observed with this inhibitor panel are specifically attributable to the inhibition of GSK-3 activity. In support of this conclusion, and as summarized in the Introduction, others have shown previously with a model of bFGF-driven angiogenesis in the

subcutaneous space of adult mice that a kinase-dead mutant of GSK-3β enhanced angiogenesis [13]. Conversely, a constitutively active GSK-3β mutant inhibited angiogenesis [13]. Also, a constitutively active mutant of GSK-3β inhibited angiogenesis and GSK-3β inhibitors other than those used here promoted angiogenesis in models of myocardial infarction [12,14]. Similarly, in vitro, a GSK-3β kinase-dead mutant promoted capillary network formation by human umbilical vein endothelial cells on 3D basement membrane Matrigel, whereas a constitutively active GSK-3β mutant disrupted capillary network formation through degradation of β-catenin [11].

Our findings with GSK-3β inhibitors and retinal MVECs undergoing capillary morphogenesis in vitro suggest that moderate inhibition of GSK-3β improves retinal neovascularization in vivo by improving the quality of pre-capillary cords, including the stability of β-catenin and the integrity cell/cell junctions during cord formation. In particular, our in vitro data suggest that GSK-3β inhibition can increase vascular cord integration by reducing blind ends. These in vitro observations demonstrating improved integration of vascular cords and improved integrity of cell/cell junctions are each consistent with the improved neovascular architecture and reduced vascular leak observed in the retinas of animals treated with GSK-3β inhibitors.

Our findings that hypoxia increases GSK-3β activity in retinal MVECs and that GSK-3β inhibitors improve functional neovascularization of hypoxic retina also suggest the hypothesis that GSK-3β is inappropriately regulated in ischemic retinopathy. Although not explored extensively, hypoxia has been linked in some circumstances to suppression of phosphatidylinositol 3′-kinase/Akt signaling, thereby resulting in the activation of GSK-3β [32]. Indeed, if GSK-3β is activated by retinal ischemia, as predicted by our in vitro experiments, improved neovascularization and oxygenation achieved with administration of moderate doses of GSK-3β inhibitors should facilitate the return GSK-3β activity to normal levels.

For the treatment of diabetes, GSK-3β inhibitors have generated considerable interest because insulin is a natural inhibitor of GSK-3β activity and because expression and activity of GSK-3 isoforms can be elevated in diabetics. Furthermore, GSK-3 activity interferes with insulin signaling by suppressing the action of insulin receptor substrate-1 and thereby may contribute to insulin resistance (reviewed in [10]). Also, GSK-3β inhibitors offer promise for treating a variety of neurodegenerative conditions [33]. The connection between GSK-3β and neuro-degeneration likely involves tau proteins; hyper-phosphorylation of tau by GSK-3β renders tau unable to interact with and stabilize microtubules and promotes neurofibrillary tangle development [10]. Thus, it seems that over-exuberant GSK-3 activity may be common to a variety of important pathologies, including diabetes, neuro-degeneration, and ischemic retinopathies. GSK-3 activity may also relate directly to diabetic retinopathy when ischemia is involved [2,31].

Finally, it is important to emphasize that the GSK-3β inhibitor strategy described here reduces the vascular pathology that damages retina without inhibiting neovascularization. Most importantly, it also alleviates hypoxia that drives abnormal neovascularization and destroys photoreceptors and ganglion cells. Thus, this GSK-3β inhibitor strategy illustrates a potentially important treatment paradigm designed to achieve vascular improvement and reduce hypoxia rather than inhibit neovascularization.

Acknowledgments

References

1. Chen J, Smith LE. Retinopathy of prematurity. Angiogenesis. 2007; 10(2):133–140. [PubMed: 17332988]

2. Gariano RF, Gardner TW. Retinal angiogenesis in development and disease. Nature. 2005; 438(7070):960–966. [PubMed: 16355161]

3. Campochiaro PA. Retinal and choroidal neovascularization. J Cell Physiol. 2000; 184(3):301–310. [PubMed: 10911360]

4. Frank RN. Diabetic retinopathy. N Engl J Med. 2004; 350(1):48–58. [PubMed: 14702427]

5. Boulton M, Foreman D, Williams G, McLeod D. Vegf localisation in diabetic retinopathy. Br J Ophthalmol. 1998; 82(5):561–568. [PubMed: 9713066]

6. Miller JW, Adamis AP, Shima DT, D'Amore PA, Moulton RS, O'Reilly MS, Folkman J, Dvorak HF, Brown LF, Berse B, et al. Vascular endothelial growth factor/vascular permeability factor is temporally and spatially correlated with ocular angiogenesis in a primate model. Am J Pathol. 1994; 145(3):574–584. [PubMed: 7521577]

7. Pierce EA, Avery RL, Foley ED, Aiello LP, Smith LE. Vascular endothelial growth factor/vascular permeability factor expression in a mouse model of retinal neovascularization. Proc Natl Acad Sci U S A. 1995; 92(3):905–909. [PubMed: 7846076]

8. Nagy JA, Senger DR. Vegf-a, cytoskeletal dynamics, and the pathological vascular phenotype. Exp Cell Res. 2006; 312(5):538–548. [PubMed: 16310771]

9. Forde JE, Dale TC. Glycogen synthase kinase 3: a key regulator of cellular fate. Cell Mol Life Sci. 2007; 64(15):1930–1944. [PubMed: 17530463]

10. Cohen P, Goedert M. Gsk3 inhibitors: development and therapeutic potential. Nat Rev Drug Discov. 2004; 3(6):479–487. [PubMed: 15173837]

11. Skurk C, Maatz H, Rocnik E, Bialik A, Force T, Walsh K. Glycogen-synthase kinase3beta/beta-catenin axis promotes angiogenesis through activation of vascular endothelial growth factor signaling in endothelial cells. Circ Res. 2005; 96(3):308–318. [PubMed: 15662032]

12. Kaga S, Zhan L, Altaf E, Maulik N. Glycogen synthase kinase-3beta/beta-catenin promotes angiogenic and anti-apoptotic signaling through the induction of vegf, bcl-2 and survivin expression in rat ischemic preconditioned myocardium. J Mol Cell Cardiol. 2006; 40(1):138–147. [PubMed: 16288908]

13. Kim HS, Skurk C, Thomas SR, Bialik A, Suhara T, Kureishi Y, Birnbaum M, Keaney JF Jr, Walsh K. Regulation of angiogenesis by glycogen synthase kinase-3beta. J Biol Chem. 2002; 277(44): 41888–41896. [PubMed: 12167628]

14. Yao YY, Yin H, Shen B, Smith RS Jr, Liu Y, Gao L, Chao L, Chao J. Tissue kallikrein promotes neovascularization and improves cardiac function by the akt-glycogen synthase kinase-3beta pathway. Cardiovasc Res. 2008; 80(3):354–364. [PubMed: 18689794]

15. Kumar A, Hou X, Lee C, Li Y, Maminishkis A, Tang Z, Zhang F, Langer HF, Arjunan P, Dong L, Wu Z, Zhu LY, Wang L, Min W, Colosi P, Chavakis T, Li X. Platelet-derived growth factor-dd targeting arrests pathological angiogenesis by modulating glycogen synthase kinase-3beta phosphorylation. J Biol Chem. 2010; 285(20):15500–15510. [PubMed: 20231273]

16. Smith LE, Wesolowski E, McLellan A, Kostyk SK, D'Amato R, Sullivan R, D'Amore PA. Oxygen-induced retinopathy in the mouse. Invest Ophthalmol Vis Sci. 1994; 35(1):101–111. [PubMed: 7507904]

17. D'Amato R, Wesolowski E, Smith LE. Microscopic visualization of the retina by angiography with high-molecular-weight fluorescein-labeled dextrans in the mouse. Microvasc Res. 1993; 46(2): 135–142. [PubMed: 7504160]

18. Connor KM, SanGiovanni JP, Lofqvist C, Aderman CM, Chen J, Higuchi A, Hong S, Pravda EA, Majchrzak S, Carper D, Hellstrom A, Kang JX, Chew EY, Salem N Jr, Serhan CN, Smith LE. Increased dietary intake of omega-3-polyunsaturated fatty acids reduces pathological retinal angiogenesis. Nat Med. 2007; 13(7):868–873. [PubMed: 17589522]

19. Hoang MV, Senger DR. In vivo and in vitro models of mammalian angiogenesis. Methods Mol Biol. 2005; 294:269–285. [PubMed: 15576918]

20. Smith LE, Shen W, Perruzzi C, Soker S, Kinose F, Xu X, Robinson G, Driver S, Bischoff J, Zhang B, Schaeffer JM, Senger DR. Regulation of vascular endothelial growth factor-dependent retinal neovascularization by insulin-like growth factor-1 receptor. Nat Med. 1999; 5(12):1390–1395. [PubMed: 10581081]

21. Senger DR, Perruzzi CA, Streit M, Koteliansky VE, de Fougerolles AR, Detmar M. The alpha(1)beta(1) and alpha(2)-beta(1) integrins provide critical support for vascular endothelial growth factor signaling, endothelial cell migration, and tumor angiogenesis. Am J Pathol. 2002; 160(1):195–204. [PubMed: 11786413]

22. Doble BW, Woodgett JR. Gsk-3: tricks of the trade for a multi-tasking kinase. J Cell Sci. 2003; 116(Pt 7):1175–1186. [PubMed: 12615961]

23. Bhat R, Xue Y, Berg S, Hellberg S, Ormo M, Nilsson Y, Radesater AC, Jerning E, Markgren PO, Borgegard T, Nylof M, Gimenez-Cassina A, Hernandez F, Lucas JJ, Diaz-Nido J, Avila J. Structural insights and biological effects of glycogen synthase kinase 3-specific inhibitor ar-a014418. J Biol Chem. 2003; 278(46):45937–45945. [PubMed: 12928438]

24. Whelan MC, Senger DR. Collagen i initiates endothelial cell morphogenesis by inducing actin polymerization through suppression of cyclic amp and protein kinase a. J Biol Chem. 2003; 278(1):327–334. [PubMed: 12399469]

25. Hoang MV, Whelan MC, Senger DR. Rho activity critically and selectively regulates endothelial cell organization during angiogenesis. Proc Natl Acad Sci U S A. 2004; 101(7):1874–1879. [PubMed: 14769914]

26. Martinez A, Alonso M, Castro A, Perez C, Moreno FJ. First non-atp competitive glycogen synthase kinase 3 beta (gsk-3beta) inhibitors: thiadiazolidinones (tdzd) as potential drugs for the treatment of alzheimer's disease. J Med Chem. 2002; 45(6):1292–1299. [PubMed: 11881998]

27. Plotkin B, Kaidanovich O, Talior I, Eldar-Finkelman H. Insulin mimetic action of synthetic phosphorylated peptide inhibitors of glycogen synthase kinase-3. J Pharmacol Exp Ther. 2003; 305(3):974–980. [PubMed: 12626660]

28. Shima DT, Adamis AP, Ferrara N, Yeo KT, Yeo TK, Allende R, Folkman J, D'Amore PA. Hypoxic induction of endothelial cell growth factors in retinal cells: Identification and characterization of vascular endothelial growth factor (vegf) as the mitogen. Mol Med. 1995; 1(2): 182–193. [PubMed: 8529097]

29. Pe'er J, Shweiki D, Itin A, Hemo I, Gnessin H, Keshet E. Hypoxia-induced expression of vascular endothelial growth factor by retinal cells is a common factor in neovascularizing ocular diseases. Lab Invest. 1995; 72(6):638–645. [PubMed: 7540233]

30. Robinson GS, Pierce EA, Rook SL, Foley E, Webb R, Smith LE. Oligodeoxynucleotides inhibit retinal neovascularization in a murine model of proliferative retinopathy. Proc Natl Acad Sci U S A. 1996; 93(10):4851–4856. [PubMed: 8643492]

31. Wangsa-Wirawan ND, Linsenmeier RA. Retinal oxygen: fundamental and clinical aspects. Arch Ophthalmol. 2003; 121(4):547–557. [PubMed: 12695252]

32. Loberg RD, Vesely E, Brosius FC 3rd. Enhanced glycogen synthase kinase-3beta activity mediates hypoxia-induced apoptosis of vascular smooth muscle cells and is prevented by glucose transport and metabolism. J Biol Chem. 2002; 277(44):41667–41673. [PubMed: 12200436]

33. Medina M, Castro A. Glycogen synthase kinase-3 (gsk-3) inhibitors reach the clinic. Curr Opin Drug Discov Devel. 2008; 11(4):533–543.
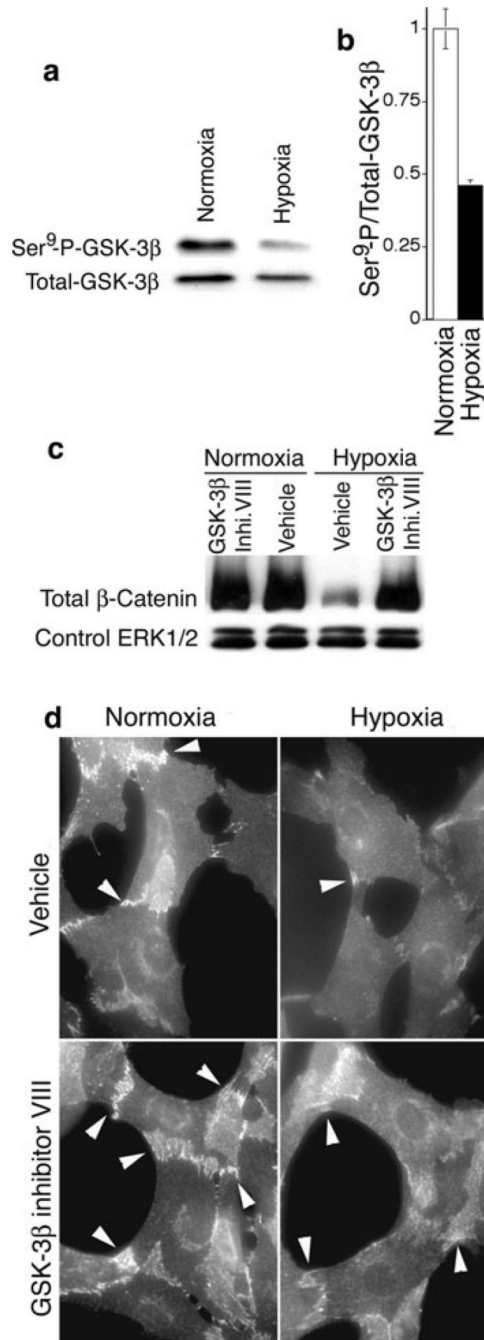
Fig. 1.
Hypoxia activates GSK-3β in retinal MVECs and decreases β-catenin. **a** Retinal MVECs were subjected to hypoxia (5% oxygen) for 6 h and analyzed for GSK-3β activity with immunoblotting. Reduced phosphorylation of Ser[9] corresponds to increased GSK-3β activity (see text). **b** Digital quantification of reduced Ser[9] phosphorylation (i.e. increased GSK-3β activity) normalized to total GSK-3β; $P < 0.01$, $n = 5$. **c** Immunoblot analyses of β-catenin in retinal MVECs subjected to hypoxia (5% oxygen) for 6 h. Where indicated, GSK-3β inhibitor VIII was added (0.5 μM). Erk1/2 staining served as a loading control (see Methods). **d** Immunostaining of β-catenin in retinal MVECs induced to undergo capillary morphogenesis with collagen-I overlay (see Methods). Where indicated, cells were

subjected to hypoxia, as above, and treated with GSK-3β inhibitor VIII (0.5 μM). β-catenin staining was particularly prominent at cell/cell junctions (*arrows*). Bar = 25 microns
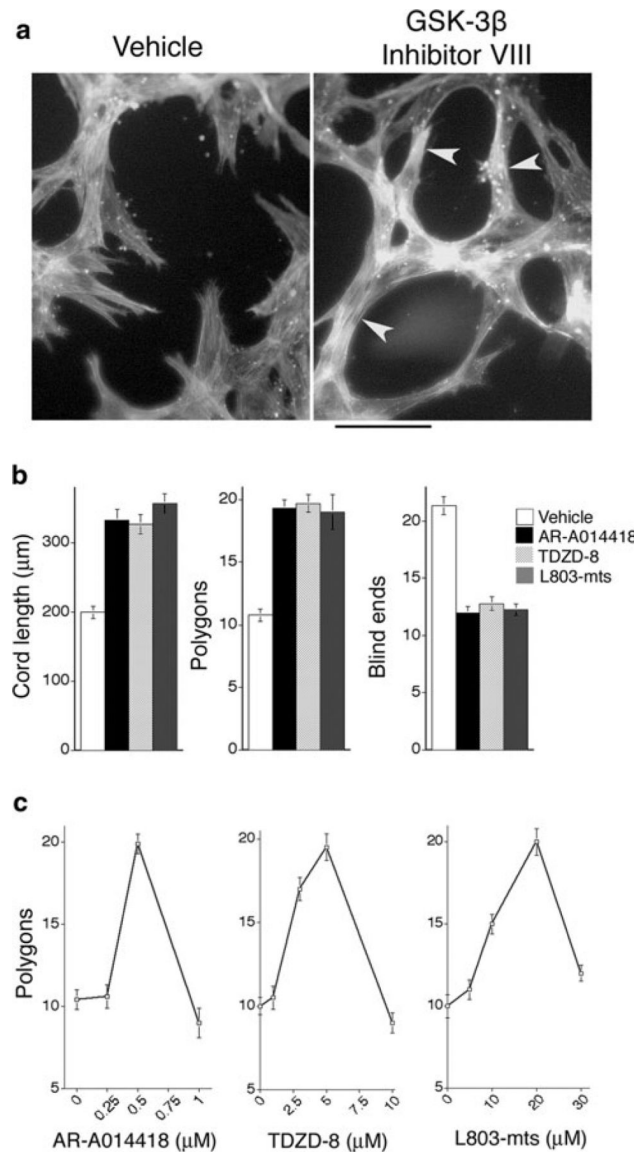
Fig. 2.
GSK-3β inhibitors improve the formation of capillary cords in vitro. **a** Capillary morphogenesis of retinal MVECs in response to "sandwiching" with 3D collagen-I; cells were stained for F-actin with FITC-phalloidin (bar = 50 microns). Note improved cord formation with GSK-3β inhibitor VIII (*right panel, arrows*). **b** Quantification of parameters that characterize capillary organization. Improved organization is reflected by increased cord length, increased numbers of inter-connected polygon networks, and reduced number of blind ends. AR-A014418 (GSK-3β inhibitor VIII) at 0.5 μM, TDZD-8 (GSK-3β inhibitor I) at 5 μM, and L803-mts (GSK-3β peptide inhibitor) at 20 μM similarly improved organization; $P < 0.001$ for each drug and each parameter, relative to control, with $n \geq 15$ for each group. Apart from optimal dose, no significant differences were observed among the inhibitors. **c** Dose-response curves for each of the inhibitors; $n \geq 9$
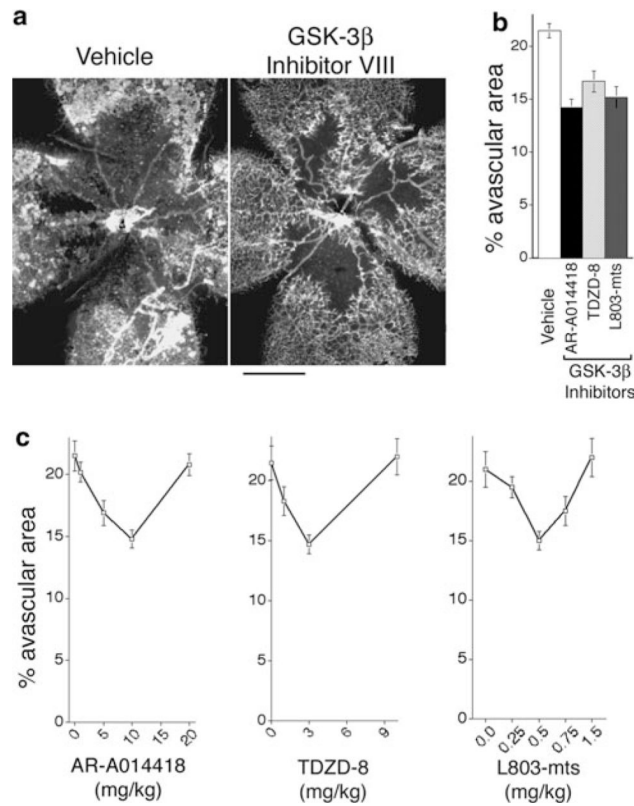
Fig. 3.
GSK-3β inhibitors improve re-vascularization in ischemic retina. Beginning with the onset of retinopathy (P12), animals were treated for 5 days with GSK-3β inhibitors. **a** Whole mount retina vasculature at P17 was stained with *Bandeiraea simplicifolia* TRITC-lectin (bar = 500 microns). **b** Quantification of % avascular area following treatment with vehicle control or optimal doses of GSK-3β inhibitors AR-A014418 (GSK-3β inhibitor VIII; 10 mg/kg), TDZD-8 (GSK-3β inhibitor I; 3 mg/kg), and L803-mts (GSK-3β peptide inhibitor; 0.5 mg/kg). $P < 0.05$ for each inhibitor relative to control; $n \geq 11$ animals for each group. Apart from optimal doses, no significant differences were observed among the inhibitors. **c** Dose response curves for each of the inhibitors; $n \geq 8$ for each group
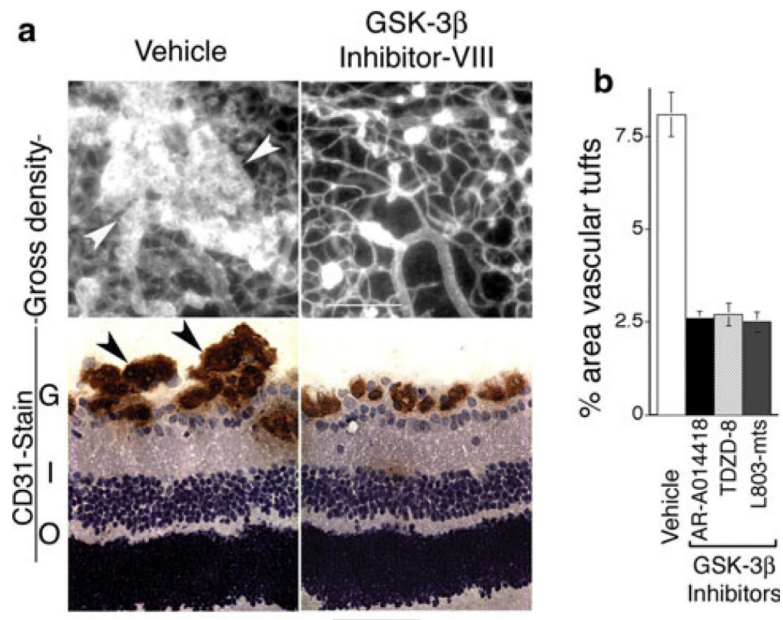
Fig. 4.
GSK-3β inhibitors reduce abnormal vascular tufts associated with ischemic retinopathy. Animals were treated with vehicle or GSK-3β inhibitors for 5 days beginning with P12 and harvested at P17. **a** *Upper panels*: whole mount retina vasculature stained with *Bandeiraea simplicifolia* TRITC-lectin. *Lower panels*: retina cross sections stained for endothelial cells with CD31 antibody. *Arrows* denote vascular tufts. *G* = ganglion layer, *I* = inner nuclear layer, *O* = outer nuclear layer. Bars: *upper panels* = 200 microns; *lower panels* = 50 microns. **b** Quantification of vascular tufts in whole mount retinas at P17: GSK-3β inhibitors AR-A014418 (GSK-3β inhibitor VIII), TDZD-8 (GSK-3β inhibitor I), and L803-mts (GSK-3β peptide inhibitor) similarly reduced the proportion of retina area containing vascular tufts ($P < 0.03$ for each inhibitor relative to vehicle controls, $n \geq 11$ animals for each group). No significant differences were observed among the inhibitors
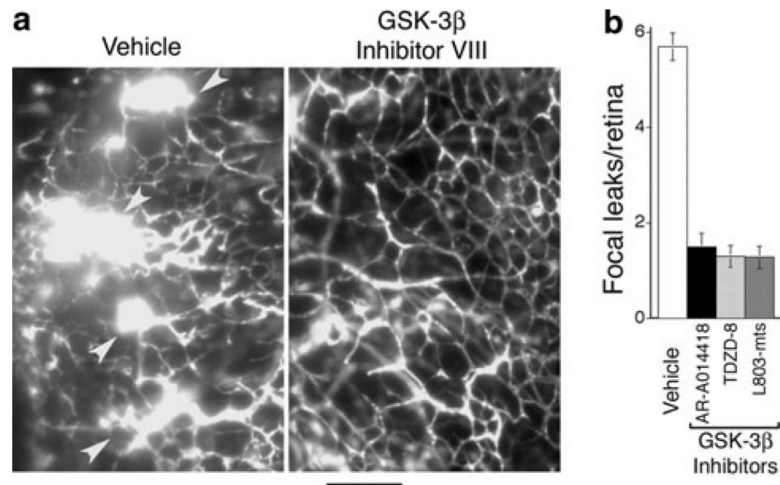
Fig. 5.
GSK-3β inhibitors reduce abnormal vascular leakage associated with retinopathy. Animals were treated with vehicle or GSK-3β inhibitors for 5 days beginning with P12 and harvested at P17. **a** *Left panel*: typical vascular leaks (*arrows*) in whole mount retina of vehicle control of animal perfused with FITC-dextran tracer. *Right panel*: typical absence of leak in whole mount retina of animal treated with GSK-3β inhibitor VIII. Bar = 100 microns. **b** Quantification of vascular leak in whole mount retinas. Relative to controls, GSK-3β inhibitors AR-A014418 (GSK-3β inhibitor VIII), TDZD-8 (GSK-3β inhibitor I), and L803-mts (GSK-3β peptide inhibitor) similarly reduced # focal leakage points/retina ($P < 0.02$ for each inhibitor relative to vehicle controls, $n \geq 13$ animals for each group). No significant differences were observed among the inhibitors
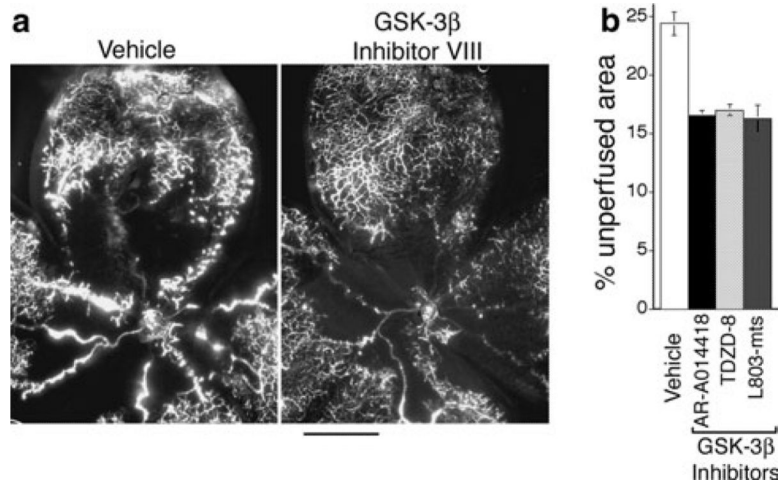
Fig. 6.
GSK-3β inhibitors improve vascular perfusion of retina. Beginning with the onset of retinopathy (P12), animals were treated for 5 days with GSK-3β inhibitors as indicated and harvested at P17. **a** Whole mounted retinal vasculature following live perfusion with FITC-dextran (bar = 500 microns). **b** Quantification of % non-perfused area following treatment with vehicle control or GSK-3β inhibitors. *P* < 0.05 for each inhibitor relative to vehicle control; *n* ≥ 11 animals for each group
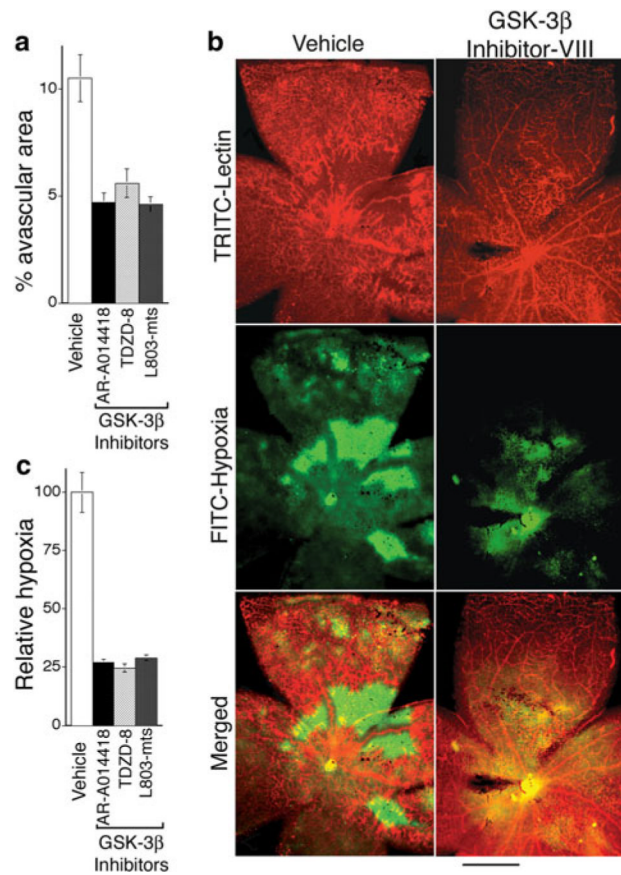
Fig. 7.
GSK-3β inhibitors accelerate reduction in retinal hypoxia. **a** Animals were treated with vehicle or GSK-3β inhibitors daily beginning with P12, harvested at P21, and avascular area quantified as in Fig. 2. GSK-3β inhibitors AR-A014418 (GSK-3β inhibitor VIII), TDZD-8 (GSK-3β inhibitor I), and L803-mts (GSK-3β peptide inhibitor) each similarly reduced avascular area relative to controls ($P < 0.02$, $n \geq 9$ animals for each group). **b** Whole mount retina vasculature at P21 was stained with *Bandeiraea simplicifolia* TRITC-lectin (*upper panels*) and for hypoxia with Hypoxyprobe™ (*middle panels*). *Bottom panels* are merged images of the *upper two panels*; bar = 500 microns. Note marked reduction in hypoxia in retina of GSK-3β inhibitor-treated animal. **c** Quantification of reduction in hypoxic area achieved with GSK-3β inhibitors at P21; $P < 0.03$ for each inhibitor relative to controls, $n \geq 11$ animals for each group. No significant differences were observed among the inhibitors